Phage-Mediated Acquisition of a Type III Secreted Effector Protein Boosts Growth of *Salmonella* by Nitrate Respiration

Christopher A. Lopez, Sebastian E. Winter, Fabian Rivera-Chávez, Mariana N. Xavier, Victor Poon, Sean-Paul Nuccio, Renée M. Tsolis, and Andreas J. Bäumler

Department of Medical Microbiology and Immunology, School of Medicine, University of California, Davis, California, USA

ABSTRACT **Information on how emerging pathogens can invade and persist and spread within host populations remains sparse. In the 1980s, a multidrug-resistant *Salmonella enterica* serotype Typhimurium clone lysogenized by a bacteriophage carrying the *sopE* virulence gene caused an epidemic among cattle and humans in Europe. Here we show that phage-mediated horizontal transfer of the *sopE* gene enhances the production of host-derived nitrate, an energetically highly valuable electron acceptor, in a mouse colitis model. In turn, nitrate fuels a bloom of *S.* Typhimurium in the gut lumen through anaerobic nitrate respiration while suppressing genes for the utilization of energetically inferior electron acceptors such as tetrathionate. Through this mechanism, horizontal transfer of *sopE* can enhance the fitness of *S.* Typhimurium, resulting in its significantly increased abundance in the feces.**

IMPORTANCE **During gastroenteritis, *Salmonella enterica* serotype Typhimurium can use tetrathionate respiration to edge out competing microbes in the gut lumen. However, the concept that tetrathionate respiration confers a growth benefit in the inflamed gut is not broadly applicable to other host-pathogen combinations because tetrathionate respiration is a signature trait used to differentiate *Salmonella* serotypes from most other members of the family *Enterobacteriaceae*. Here we show that by acquiring the phage-carried *sopE* gene, *S.* Typhimurium can drive the host to generate an additional respiratory electron acceptor, nitrate. Nitrate suppresses genes for the utilization of energetically inferior electron acceptors such as tetrathionate while enhancing the luminal growth of *S.* Typhimurium through anaerobic nitrate respiration. Pathways for anaerobic nitrate respiration are widely conserved among members of the family *Enterobacteriaceae*, thereby making our observations relevant to other enteric pathogens whose relative abundance in the intestinal lumen increases during infection.**

Received 7 May 2012 **Accepted** 24 May 2012 **Published** 12 June 2012

Citation Lopez CA, et al. 2012. Phage-mediated acquisition of a type III secreted effector protein boosts growth of *Salmonella* by nitrate respiration. mBio 3(3):e00143-12. doi: 10.1128/mBio.00143-12.

Editor Stanley Maloy, San Diego State University

Address correspondence to Andreas J. Bäumler, ajbaumler@ucdavis.edu.

The first human outbreak of a multidrug-resistant (MDR) pathogen was recorded between 1964 and 1966 in Great Britain (1). The outbreak was caused by a *Salmonella enterica* serotype Typhimurium strain which circulated in cattle and had acquired resistance to furazolidone, ampicillin, chloramphenicol (Cm), kanamycin (Kan), neomycin, streptomycin, sulfonamides, and tetracyclines. Differentiation of *S.* Typhimurium isolates by phage typing identified the outbreak strain as a distinct clone with definitive phage type 29 (DT29) (1). Subsequent surveillance by the Central Veterinary Laboratory in the United Kingdom revealed the emergence of several MDR clones over time. Each epidemic clone, after dominating for a period of time in its bovine animal reservoir, was eventually replaced, as indicated by the dominance of a new phage type (reviewed in reference 2). However, the rise and fall of epidemic *S.* Typhimurium phage types were not accompanied by obvious changes in their antibiotic resistance profiles, suggesting that antibiotic resistance is not the sole property that enhances the fitness of a newly emergent clone.

Phage types DT204 and DT204c define an epidemic MDR *S.* Typhimurium clone which dominated in Europe in the 1980s (2). Isolates of this clone are lysogenized by a bacteriophage, termed SopEΦ, which carries the *sopE* virulence gene (3, 4). The SopEΦ prophage is present in only a small fraction of *S.* Typhimurium isolates, including phage types DT204, DT204c, and DT49 and laboratory strain SL1344 (4). Based on the association of SopEΦ with an epidemic *S.* Typhimurium clone, it has been speculated that acquisition of the SopE protein by phage-mediated horizontal gene transfer might have increased the fitness of the resulting strain in its host population (5). However, experimental evidence for this hypothesis is lacking.

The *sopE* gene encodes a secreted substrate (effector protein) of the invasion-associated type III secretion system (T3SS-1) of *S.* Typhimurium (3, 6). SopE activates several innate immune signaling pathways (6–8) and is a potent inducer of intestinal inflammation (9, 10), but the molecular mechanisms by which SopE might enhance the fitness of an epidemic *S.* Typhimurium clone remain unknown. Here we investigated whether SopE increases the fitness of *S.* Typhimurium in a mouse colitis model and elucidated the underlying mechanism.

RESULTS

SopE enhances growth in the inflamed intestine. The *sopE* gene increases the severity of intestinal inflammation (8, 10), and this host response enhances the luminal growth of *S.* Typhimurium

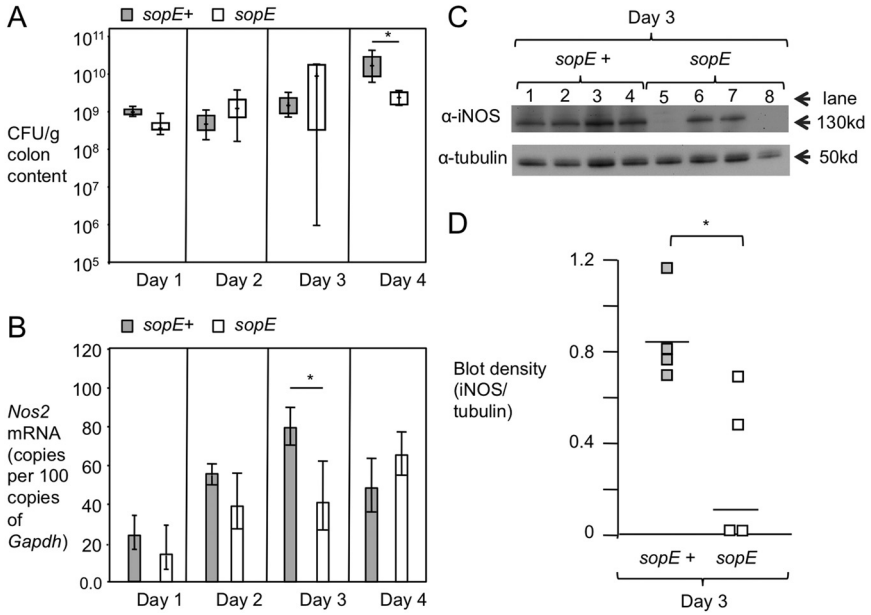

FIG 1 The *sopE* gene induces iNOS expression and enhances the growth of *S.* Typhimurium in the intestine. Groups of streptomycin-pretreated mice were infected with the SL1344 wild type (CAL63, *sopE*$^+$) or a *sopE* mutant (CAL88, *sopE*). Groups of mice were euthanized at the indicated time points. For all groups, $n = 4$ except for the day 2 *sopE*$^+$ group ($n = 3$) (a) Analysis of bacterial numbers in the colon contents. Boxes in whisker plots represent the second and third quartiles, while lines indicate the first and fourth quartiles. (B) *Nos2* mRNA levels in the mucosa were quantified by real-time PCR. Bars represent geometric mean *Nos2* copy numbers per 100 copies of glyceraldehyde 3-phosphate dehydrogenase (*Gapdh*) mRNA ± the standard errors. (C) Levels of iNOS protein in the mucosa from mice infected with *sopE*$^+$ (lanes 1 to 4) or *sopE* mutant (lanes 5 to 8) strains were determined by Western blotting (top panel). Detection of tubulin by Western blotting served as a loading control (bottom panel). Each lane represents protein extracts isolated from one animal. Molecular masses of standard proteins are indicated on the right. (D) Quantification of iNOS levels in Western blot assays by densitometry. Each square represents the intensity of the iNOS signal divided by the intensity of the tubulin signal from one animal. Significance is based on the two-tailed Student *t* test. *, $P < 0.05$.

(11, 12). Based on these observations, we reasoned that SopE might increase the bacterial numbers in the gut contents. We used *S.* Typhimurium strain SL1344 (13), which carries the SopEΦ prophage (3), to investigate whether acquisition of the *sopE* gene enhances the fitness of the pathogen in the mouse colitis model (14). In this model, genetically susceptible mice (C57BL/6) are given streptomycin 24 h prior to *S.* Typhimurium administration. Treatment of mice with streptomycin prior to bacterial inoculation disrupts the resident microbiota to allow *S.* Typhimurium to elicit a pathology similar to human gastroenteritis (14). A previous study found the SL1344 wild type and a derivative carrying mutations in *invG* (resulting in inactivation of T3SS-1) and *sseD* (resulting in inactivation of T3SS-2) are recovered in equal numbers from intestinal contents during the first 3 days after infection in the mouse colitis model (12). However, at day 4 after infection, mice infected with the SL1344 wild type, which elicits intestinal inflammation, contain significantly higher numbers of *S.* Typhimurium bacteria in their intestinal contents than mice infected with an *invG sseD* mutant which does not elicit intestinal inflammation (12). To determine whether *sopE* contributes to this inflammation-induced growth advantage, we used groups of mice (C57BL/6) preconditioned by treatment with streptomycin and infected with an SL1344 strain marked with an antibiotic resistance cassette (*phoN*::Kan, CAL63), here referred to as the wild type, or with an isogenic mutant lacking the *sopE* gene (*phoN*::Kan Δ*sopE*, CAL88). Four days after infection, the colon contents of mice infected with the *sopE*-carrying wild-type strain (CAL63) contained significantly higher numbers ($P < 0.05$) of *S.* Typhimurium than the colon contents of mice infected with the isogenic *sopE* mutant (CAL88) (Fig. 1A), suggesting that the presence of SopE significantly enhances the ability of *S.* Typhimurium SL1344 to grow in the intestinal lumen. This is the first time SopE has been shown to enhance luminal growth of *S.* Typhimurium in the inflamed gut.

SopE enhances iNOS expression. One mechanism by which *S.* Typhimurium can edge out competing microbes in the inflamed intestine is growth by anaerobic tetrathionate respiration (15). To test whether SopE enhances the growth advantage conferred by tetrathionate respiration, we infected streptomycin-pretreated mice (C57BL/6) with an equal mixture of the SL1344 wild type (CAL63) and an isogenic mutant defective for tetrathionate respiration (*ttrA* mutant, CAL66). Surprisingly, both strains were recovered in similar numbers from colon contents 4 days after infection (data not shown), indicating that tetrathionate respiration did not enhance the luminal growth of an *S.* Typhimurium SopEΦ lysogen. Similar results were obtained with genetically resistant (CBA/J) mice, which develop intestinal inflammation slowly, within 1 to 2 weeks after *S.* Typhimurium infection in the absence of streptomycin pretreatment. The *S.* Typhimurium SL1344 wild type (CAL63) and its isogenic *ttrA* mutant (CAL66) were recovered in similar numbers from the feces over time (see Fig. S1 in the supplemental material). In contrast, an *S.* Typhimurium strain naturally lacking the SopEΦ prophage (IR715) was recovered from fecal contents of CBA mice in significantly higher numbers than its isogenic *ttrA* mutant (SW661) starting as early as day 5 after infection and continuing throughout the remainder of the experiment (see Fig. S1 in the supplemental material).

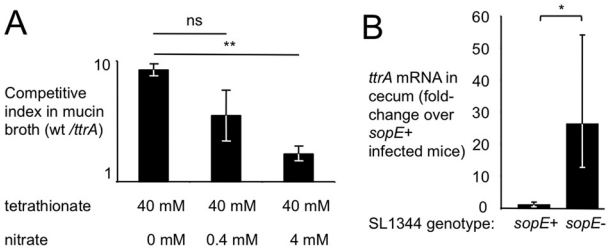

FIG 2 Inhibition of tetrathionate respiration by nitrate and SopE. (A) Mucin broth containing the indicated concentrations of nitrate and tetrathionate was inoculated with an equal mixture of the SL1344 wild-type strain (wt, CAL63) and a *ttrA* mutant (CAL66). Bacterial numbers were determined after 16 h of anaerobic growth. Bars represent geometric means of the competitive index ± the standard errors. Results are averages of three independent experiments. (B) Groups of streptomycin-pretreated mice ($n = 4$ per group) were infected with the SL1344 wild type (CAL63, *sopE*$^+$) or a *sopE* mutant (CAL88, *sopE*), and bacterial RNA was extracted from cecal contents 4 days after infection. The relative levels of *ttrA* mRNA were quantified by real-time PCR, normalized to the abundance of *S.* Typhimurium 16S rRNA, and expressed as *n*-fold differences from the *ttrA* mRNA levels present in the SL1344 wild type (CAL63, *sopE*$^+$). Bars represent geometric means ± standard errors. Significance is based on the two-tailed Student *t* test. **, $P < 0.01$; *, $P < 0.05$; ns, $P > 0.05$.

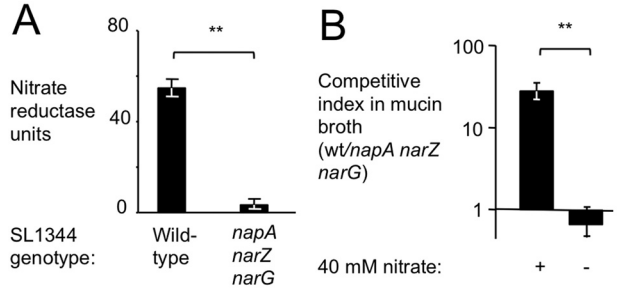

FIG 3 Inactivation of nitrate reductases in *S.* Typhimurium. (A) Detection of nitrate reductase activity in the *S.* Typhimurium wild type (SL1344) and a *narG narZ napA* mutant (CAL59). Briefly, the nitrate reductase assay measures the reduction of nitrate to nitrite with methyl viologen as an electron donor. Nitrate is added to the reaction medium containing lysed bacterial cells, and nitrite (from nitrate reductase activity) is measured on the basis of its formation of a colored azo compound, which is quantified with a spectrophotometer. (B) Mucin broth was inoculated with an equal mixture of the SL1344 wild-type strain (wt, CAL63) and a *narG narZ napA* mutant (CAL64). Competitive indices for anaerobic growth in mucin broth with (+) or without (−) nitrate are shown. Bars represent geometric means ± standard errors. The data are from three independent experiments. Significance is based on the two-tailed Student *t* test. **, $P < 0.01$.

To further characterize the role of SopE during infection, we analyzed the cecal immune response elicited by *S.* Typhimurium strain SL1344 in the mouse colitis model. We noticed that the SL1344 wild type (CAL63) induced *Nos2* gene expression at significantly higher levels than a *sopE* mutant (CAL88) at day 3 after the infection of streptomycin-pretreated C57BL/6 mice (Fig. 1B), although the *Nos2* mRNA levels in the two groups were similar at day 4 after infection. *Nos2* encodes inducible nitric oxide (NO) synthase (iNOS), which was present at significantly ($P < 0.05$) higher levels in the cecal mucosa 3 days after infection with the wild type (CAL63) than after infection with a *sopE* mutant (CAL88), as shown by immunoblotting (Fig. 1C) followed by quantification by densitometry (Fig. 1D). Thus, the SopE-mediated growth advantage observed 4 days after infection (Fig. 1A) was preceded by a SopE-mediated increase in iNOS expression at day 3 after infection (Fig. 1B to D).

Nitrate is a negative regulator of tetrathionate respiration. The activity of iNOS generates NO, which reacts with reactive oxygen species (ROS) to form peroxynitrite ($ONOO^-$), a bactericidal reactive nitrogen species that quickly isomerizes to harmless nitrate (NO_3^-) (16). Nitrate is the preferred anaerobic electron acceptor of *Salmonella* serotypes (17), presumably because the relatively high standard redox potential (E_0) of the nitrate-nitrite redox couple ($E_0 = 433$ mV) makes this electron acceptor energetically favorable over the tetrathionate-thiosulfate couple, which has a lower E_0 (170 mV) (18). To test whether the presence of nitrate is sufficient to suppress the growth advantage conferred by tetrathionate respiration, mucin broth containing tetrathionate and various concentrations of nitrate was inoculated with an equal mixture of the Kan^r SL1344 wild-type strain (CAL63) and an isogenic carbenicillin-resistant (Carb^r) *ttrA* mutant (CAL66). Addition of nitrate diminished the growth advantage conferred by tetrathionate respiration in mucin broth containing tetrathionate (Fig. 2A). These data suggested that in the presence of the energetically preferred nitrate, the growth benefit conferred by tetrathionate respiration was diminished.

SopE changes *ttrA* gene expression during infection. One possible scenario to explain the above observations is that SopE-induced expression of iNOS in the cecal mucosa generates nitrate, which in turn suppresses the expression of tetrathionate utilization genes (*ttrBAC*) in the inflamed gut. To test this idea, we extracted bacterial RNA from the intestinal contents of mice 4 days after infection with the SL1344 wild-type strain (CAL63) or with an isogenic *sopE* mutant (CAL88) (mouse colitis model). Relative levels of expression of the *ttrA* mRNA, which encodes the large subunit of the tetrathionate reductase complex, were determined by quantitative real-time PCR and normalized to the abundance of *S.* Typhimurium 16S rRNA (15). Remarkably, expression of *ttrA* was significantly lower in the SopE-expressing SL1344 wild type (CAL63) than in the *sopE* mutant (CAL88) (Fig. 2B). These data suggested that the presence of the *sopE* gene markedly reduced the expression of *ttrA* in luminal *S.* Typhimurium *in vivo*.

SopE enhances nitrate respiration-dependent growth of *S.* Typhimurium. S. Typhimurium can utilize nitrate as a terminal electron acceptor (17, 19). We therefore reasoned that the intestinal growth advantage conferred by SopE (Fig. 1A) might be due to anaerobic nitrate respiration. To test this hypothesis, we generated a nitrate respiration-deficient mutant of SL1344. Three operons, including *narGHJI*, *narZYWV*, and *napFDAGHBC*, contribute to nitrate reductase activity in *S.* Typhimurium (20, 21). We disrupted the *narG*, *narZ*, and *napA* genes in SL1344 to create a mutant (CAL55) that completely lacked respiratory nitrate reductase activity (Fig. 3A). Anaerobic coculture of the Kan^r SL1344 wild type (CAL63) with the isogenic Carb^r *narG narZ napA* mutant (CAL64) in mucin broth resulted in enrichment for the wild type when the medium was supplemented with nitrate but not when nitrate was absent (Fig. 3B).

To investigate whether nitrate respiration genes confer a growth benefit in the inflamed intestine, we used the mouse colitis model and infected C57BL/6 mice with an equal mixture of the SL1344 wild-type strain (CAL63) and the isogenic, nitrate respiration-deficient mutant (*narG narZ napA* mutant, CAL64). *S.* Typhimurium infection resulted in acute intestinal inflammation (Fig. 4A and B) and markedly increased levels of mRNAs for genes that encode proinflammatory cytokines (keratinocyte-

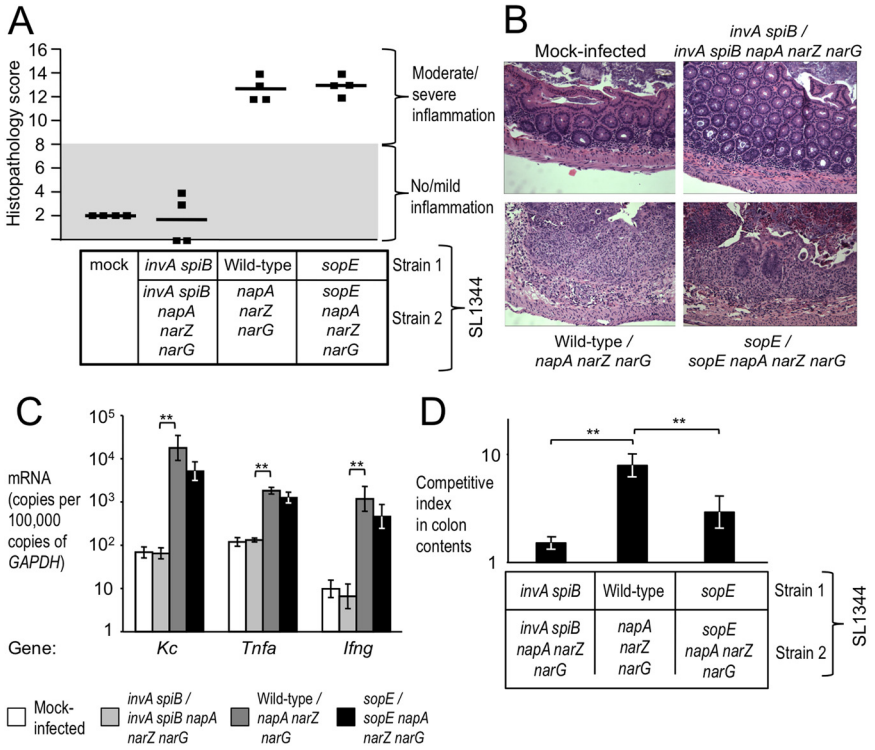

FIG 4 The *sopE* gene boosts nitrate respiration-dependent growth *in vivo*. Groups of streptomycin-pretreated mice ($n = 4$ per group) were inoculated with sterile medium (mock) or with equal mixtures of *S.* Typhimurium SL1344 derivatives (relevant genotypes are indicated), and organs were collected for analysis 4 days after infection. (A) Blinded histopathology scoring of cecal inflammation showing average scores (bars) and scores of individual animals (squares). (B) Representative images of sections from the cecal mucosa. (C) Expression of proinflammatory markers in the cecal mucosa was determined by quantitative real-time PCR analysis. Bars represent geometric mean KC-, tumor necrosis factor alpha-, and IFN-γ-encoding (*Kc*, *Tnfa*, and *Ifng*, respectively) mRNA copy numbers per 100,000 copies of glyceraldehyde 3-phosphate dehydrogenase (*GAPDH*) mRNA ± the standard errors. (D) Competitive indices of *S.* Typhimurium strains recovered from the colon contents of infected mice. Bars represent geometric means ± standard errors. Significance is based on the two-tailed Student *t* test. **, $P < 0.01$.

derived chemokine [KC], tumor necrosis factor alpha, and gamma interferon [IFN-γ]) (Fig. 4C). Four days after infection, the SL1344 wild-type strain (CAL63) was recovered in higher numbers than the *narG narZ napA* mutant (CAL64) (Fig. 4D). Similar results were obtained in the absence of streptomycin pretreatment when genetically resistant (CBA/J) mice were infected with an equal mixture of CAL63 and CAL64. Outgrowth of the nitrate respiration-competent strain (CAL63) was observed starting day 16 after infection in this model (see Fig. S2 in the supplemental material).

Interestingly, when streptomycin-pretreated C57BL/6 mice were infected with an equal mixture of a Kan^r SL1344 *sopE* mutant (CAL88) and a Carb^r *sopE narG narZ napA* mutant (CAL89), the growth advantage conferred by nitrate respiration was significantly ($P < 0.01$) diminished (Fig. 4D). Collectively, these data suggested that the presence of the *sopE* gene significantly enhanced the luminal growth advantage conferred by nitrate respiration genes.

S. Typhimurium causes intestinal inflammation by deploying T3SS-1 for epithelial invasion and T3SS-2 to promote macrophage survival (14, 22, 23). Inactivation of T3SS-1 (through a mutation in *invA*) and T3SS-2 (through a mutation in *spiB*) renders *S.* Typhimurium unable to trigger intestinal inflammation (24). To determine whether nitrate respiration supports luminal growth in the absence of inflammation, streptomycin-pretreated C57BL/6 mice were infected with an equal mixture of a Kan^r *invA spiB* mutant (CAL86) and a Carb^r *invA spiB narG narZ napA* mutant (CAL85). Mice infected with this mixture neither developed intestinal pathology (Fig. 4A and B) nor exhibited elevated levels of mRNAs for genes that encode proinflammatory cytokines (Fig. 4C). The equal recovery of both strains from colon contents 4 days after infection suggested that nitrate respiration provided little growth benefit in the absence of intestinal inflammation (Fig. 4D).

Growth of *S.* Typhimurium is driven by host-derived nitrate. To further investigate the significance of SopE-mediated induction of iNOS expression during infection (Fig. 1B to D), wild-type mice (C57BL/6) or iNOS-deficient mice (i.e., mice carrying a mutation in *Nos2*) were infected with an equal mixture of the Kan^r SL1344 wild-type strain (CAL63) and the isogenic, nitrate respiration-deficient Carb^r mutant (*narG narZ napA* mutant, CAL64). As expected, iNOS expression was detected in wild-type mice but not in iNOS-deficient mice (Fig. 5A) but both groups exhibited similarly severe pathological changes 4 days after *S.* Typhimurium infection (Fig. 5B and C). While a growth advantage of the wild type (CAL63) over the *narG narZ napA* mutant (CAL64) was observed in wild-type mice, no enrichment for the *S.* Typhimurium wild-type strain was observed in *Nos2*-deficient mice (Fig. 5D; $P < 0.01$). These data suggested that host-derived

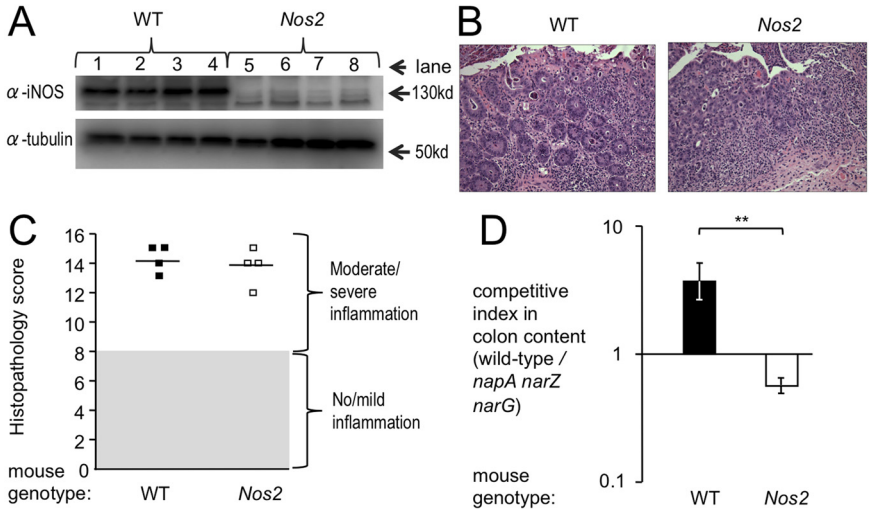

FIG 5 Nitrate driving anaerobic respiration is host derived. Groups ($n = 4$) of streptomycin-pretreated wild-type (WT) mice (C57BL/6) or iNOS-deficient mice (*Nos2*) were inoculated with an equal mixture of an *S.* Typhimurium SL1344 wild-type strain (CAL63) and a *narG narZ napA* mutant (CAL64), and organs were collected 4 days after infection. (A) Levels of mucosal iNOS protein in wild-type (lanes 1 to 4) and iNOS-deficient mice (lanes 5 to 8) were determined by Western blotting (top). Detection of tubulin by Western blotting served as a loading control (bottom). Each lane represents protein extracts isolated from one animal. Molecular masses (kilodaltons [kd]) of standard proteins are indicated on the right. (B) Representative images of sections from the cecal mucosa. (C) Blinded histopathology scoring of cecal inflammation showing average scores (bars) and scores of individual animals (squares). (D) Competitive indices of *S.* Typhimurium strains recovered from the colon contents of infected mice. Bars represent geometric means ± standard errors. Significance is based on the two-tailed Student *t* test. **, $P < 0.01$.

nitrate supports the nitrate respiration-dependent luminal growth of *S.* Typhimurium.

Horizontal transfer of the SopEΦ prophage enhances growth by nitrate respiration. SopE is encoded by a mobile genetic element, lysogenic SopEΦ, that can be transferred horizontally between different strains (5, 25). To recapitulate phage-mediated horizontal transfer of the *sopE* gene, we determined how intestinal growth of *S.* Typhimurium IR715 is altered by lysogenization with SopEΦ. We infected mice with an equal mixture of IR715 with an isogenic nitrate respiration-deficient mutant (IR715 *narG narZ napA* mutant, CAL50) (mouse colitis model). Four days after infection, mice exhibited acute intestinal inflammation (Fig. 6A and B) and elevated levels of mRNAs for genes that encode proinflammatory cytokines (Fig. 6C). Nitrate respiration conferred a small growth advantage, as indicated by the recovery of higher numbers of the *S.* Typhimurium wild type (IR715) than of the isogenic nitrate respiration-deficient mutant (IR715 *narG narZ napA* mutant, CAL50) (Fig. 6D). This nitrate respiration-dependent growth advantage was not observed in mice infected with an equal mixture of a nalidixic acid-resistant (Nal^r) IR715 *invA spiB* mutant (SPN452) and an IR715 *invA spiB narG narZ napA* $Carb^r$ mutant (CAL87) (Fig. 6D), presumably because these strains failed to elicit intestinal inflammation (Fig. 6A to C).

We next infected mice with an equal mixture of IR715 carrying the SopEΦ prophage (CAL99) and an isogenic nitrate respiration-deficient mutant (IR715 SopEΦ *narG narZ napA* mutant, CAL98) (mouse colitis model). The growth benefit conferred by nitrate respiration genes was significantly ($P < 0.05$) greater in strains lysogenized by the SopEΦ prophage (CAL99 versus CAL98) than in strains lacking the SopEΦ prophage (IR715 versus, CAL50) (Fig. 6D). These data suggested that horizontal transfer of SopEΦ significantly enhanced the luminal growth advantage conferred by nitrate respiration in the mouse colitis model. To exclude the possibility that other genes carried by the SopEΦ prophage contributed to the enhancement of *S.* Typhimurium growth by nitrate respiration, we repeated the experiment after deleting the *sopE* gene. Mice were infected with an equal mixture of IR715 carrying a SopEΦ prophage derivative in which the *sopE* gene had been deleted (IR715 SopEΦ Δ*sopE* mutant, CAL102) and an isogenic nitrate respiration-deficient mutant (IR715 SopEΦ Δ*sopE narG narZ napA* mutant, CAL103) (mouse colitis model). Deletion of the *sopE* gene (CAL102 versus CAL103) reduced the luminal growth advantage conferred by nitrate respiration to levels observed in strains lacking the SopEΦ prophage (IR715 versus, CAL50) (Fig. 6D). The reduced competitive advantage was not due to lessened inflammation, as both the histopathology scores and levels of inflammatory cytokines of the groups were similar (Fig. 6A to C).

Taken together, these results indicated that SopEΦ-mediated horizontal transfer of the *sopE* gene could increase the luminal abundance of *S.* Typhimurium by boosting growth through nitrate respiration.

DISCUSSION

SopE is a T3SS-1 effector protein (26) that enhances intestinal inflammation during *S.* Typhimurium infection (9, 10) by activating caspase 1, which in turn cleaves the immature forms of interleukin-1β (IL-1β) and IL-18 into biologically active cytokines (7, 8). During *S.* Typhimurium infection, IL-18 contributes to the early production of IFN-γ (27), a cytokine that is a potent inducer of iNOS expression (28–31). Here we show that the presence of the *sopE* gene resulted in a significant increase in mucosal iNOS production 3 days after *S.* Typhimurium infection in the mouse colitis model. NO generated by iNOS can react with ROS to form peroxynitrite ($ONOO^-$), which isomerizes to nitrate

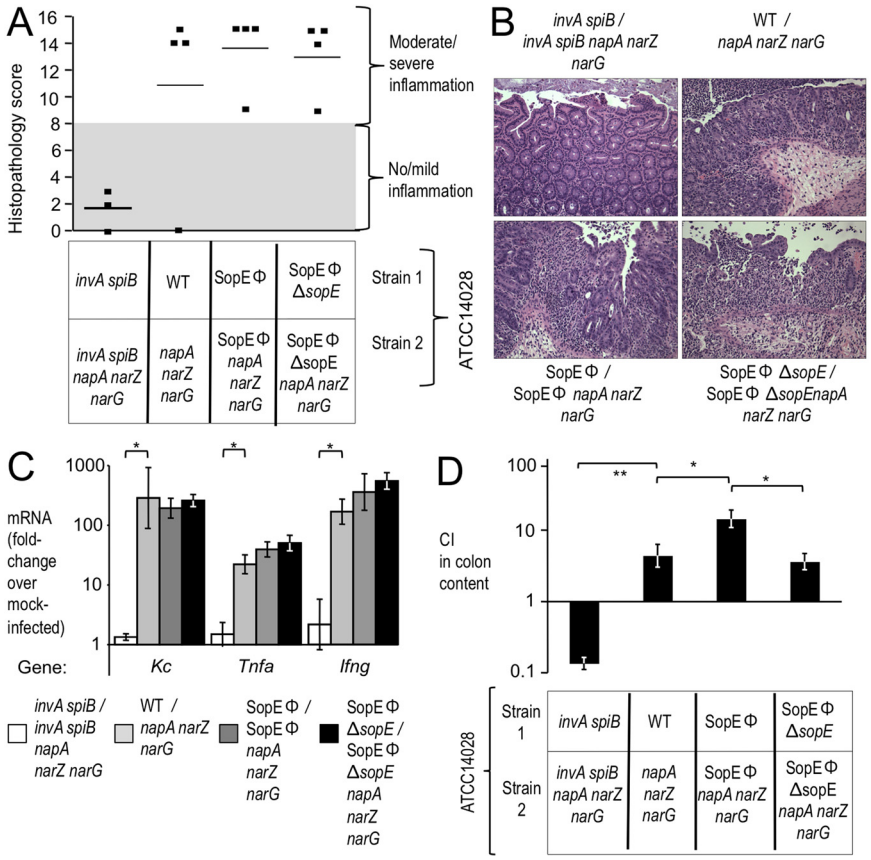

FIG 6 Horizontal transfer of the SopEΦ prophage boosts nitrate respiration-dependent growth *in vivo*. Groups of streptomycin-pretreated mice (the number of mice in each group is shown in panel A) were inoculated with sterile medium (mock) or with equal mixtures of *S.* Typhimurium ATCC 14028 derivatives (relevant genotypes are indicated), and organs were collected for analysis 4 days after infection. (A) Blinded histopathology scoring of cecal inflammation showing average scores (bars) and scores of individual animals (squares). (B) Representative images of sections from the cecal mucosa. (C) Expression of proinflammatory markers in the cecal mucosa was determined by quantitative real-time PCR analysis. Bars represent geometric means of *n*-fold changes in KC-, tumor necrosis factor alpha-, and IFN-γ-encoding (*Kc*, *Tnfa*, and *Ifng*, respectively) mRNA levels over mRNA levels in mock-infected mice ± the standard errors. (D) Competitive indices (CI) of *S.* Typhimurium strains recovered from the colon contents of infected mice. Bars represent geometric means ± standard errors. Significance is based on the two-tailed Student *t* test. *, $P < 0.05$; **, $P < 0.01$. WT, wild type.

(NO_3^-) (16), a terminal electron acceptor that can promote the growth of *S.* Typhimurium by anaerobic nitrate respiration (17, 19). The elevated mucosal iNOS production observed 3 days after infection was followed the next day by a nitrate respiration-dependent luminal growth advantage of *sopE*-positive *S.* Typhimurium. This nitrate respiration-dependent luminal growth advantage was abrogated in iNOS-deficient mice. The picture emerging from these data is that SopE-dependent iNOS expression generates host-derived nitrate, which in turn boosts the luminal growth of *S.* Typhimurium in the inflamed intestine through nitrate respiration (Fig. 7).

The *sopE* gene is carried by a bacteriophage, termed SopEΦ (3), that is absent from most *S.* Typhimurium isolates (4). The presence of SopEΦ in an *S.* Typhimurium clone that caused an epidemic in cattle and humans in Europe in the 1980s suggests that the fitness of this epidemic clone might have been increased by phage-mediated horizontal transfer of the *sopE* gene (5). Here we show that transfer of SopEΦ into a SopE-negative *S.* Typhimurium isolate (ATCC 14028) increased its fitness by conferring a nitrate respiration-dependent luminal growth advantage.

In *Escherichia coli*, genes for anaerobic respiration are subject to a hierarchical control that ensures that the respiratory electron acceptor with the most positive E_0 is used preferentially (32–38). The nitrate-nitrite redox couple is a terminal electron acceptor with a higher E_0 (433 mV) (39) than the tetrathionate-thiosulfate couple (E_0 = 170 mV) (18). Here we show that nitrate is a negative regulator of anaerobic tetrathionate respiration *in vitro*. Furthermore, the presence of the *sopE* gene significantly reduced the expression of tetrathionate respiration genes in the luminal *S.* Typhimurium population *in vivo*. This hierarchical control of genes involved in anaerobic respiration might ensure that the energetically preferred terminal electron acceptor is used preferentially to maximize the growth rate in the competitive environment of the large bowel.

The observation that tetrathionate provides a growth advantage in the inflamed intestine (40) is not germane to host interactions of the majority of the members of the family *Enterobacteriaceae*, because tetrathionate respiration is a signature trait historically used to differentiate *Salmonella* serotypes from most other bacteria (41). In contrast, the concept that nitrate respiration can provide a growth benefit during intestinal inflammation is relevant to other host-microbe interactions, since nitrate reduc-

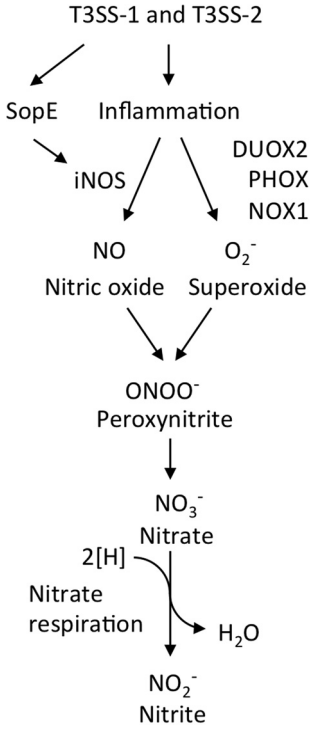

FIG 7 Model of the chain of events by which SopE boosts nitrate respiration-dependent growth of *S.* Typhimurium in the inflamed intestine. For an explanation, see the text. DUOX2, dual-oxidase 2 of epithelial cells; NOX1, NADPH oxidase 1 of epithelial cells; PHOX, NADPH oxidase of phagocytes.

tases are widely conserved among the *Proteobacteria*. For example, nitrate respiration enhances the ability of *Campylobacter jejuni* to colonize the chicken cecum (42). In the genitourinary tract, *Neisseria gonorrhoeae* has been hypothesized to use nitrite as a terminal electron acceptor to survive in anoxic environments alongside strict anaerobes (43). Finally, nitrate respiration has been postulated to contribute to the successful colonization of anoxic microenvironments in the respiratory tract by *Mycobacterium bovis* and *Pseudomonas aeruginosa* (44, 45). However, this is the first study to find a direct effect of a T3SS effector protein, SopE, in manipulating the host to provide a terminal electron acceptor for use in respiration. The degree to which other bacteria may use effector proteins or other virulence factors to manipulate host production of terminal electron acceptors will be an exciting area of future research.

MATERIALS AND METHODS

Bacterial culture conditions. For the *Escherichia coli* and *S.* Typhimurium strains used in this study, see Table S1 in the supplemental material. Strains were routinely grown in LB broth (10 g/liter tryptone, 5 g/liter yeast extract, 10 g/liter) or on LB plates (15 g/liter agar) with the appropriate antibiotic at the following concentrations: Carb, 0.1 mg/ml; Cm, 0.03 mg/ml; Kan, 0.1 mg/ml; Nal, 0.05 mg/ml; tetracycline (Tet), 0.02 mg/ml.

Transduction using phage P22. Once single mutations were obtained in an *S.* Typhimurium strain, phage lysates were generated. We incubated 1 ml of an overnight culture of the strain of interest with 4 ml of P22 broth (LB broth supplemented with 1× E minimal medium [46], 0.2% glucose, and 10^{10} to 10^{11} PFU/ml P22 *HT*-int) overnight at 37°C. Debris was removed by centrifugation at 10,000 × *g* for 5 min, and the phage-containing supernatant was mixed with chloroform (20% final volume) and stored at 4°C. To transfer mutations between strains, diluted phage lysate containing the mutation of interest was incubated for 1 h at room temperature with an overnight culture of the recipient bacterial strain. The bacteria were then spread onto plates with the appropriate antibiotic. Resulting colonies were streaked onto Evans blue uranine agar plates (10 g/liter tryptone, 5 g/liter yeast extract, 5 g/liter NaCl, 2.5 g glucose, 15 g/liter Difco agar, 0.00125% Evans blue solution, 0.5% K_2HPO_4, 0.0025% sodium fluorescein) to select for nonlysogenic colonies. The sensitivity of the resulting strains to reinfection with P22 was determined by cross-streaking of the bacterial strain with P22 H5.

Construction of *S.* Typhimurium mutants. To construct the *napA* mutant CAL46, as well as the *narZ* mutant CAL40, approximately 1-kb regions upstream and downstream of either *napA* or *narZ* were PCR amplified (see Table S2 in the supplemental material) and digested with XbaI (New England Biolabs). The two regions flanking each target gene were ligated and PCR amplified to obtain an approximately 2-kb region that was inserted into pCR2.1 with a TOPO cloning kit (Invitrogen), creating plasmids pCAL3 and pCAL1, respectively. The insertions were then sequenced. The plasmids were next digested with SphI to excise the *napA* or *narZ* flanking regions, which were then inserted into suicide plasmid pRDH10 to obtain pCAL9 and pCAL10, respectively. These plasmids were propagated in *E. coli* DH5α λ*pir*. A Kan^r cassette from pUCKSAC was inserted into the XbaI restriction site between the flanking regions to create pCAL11 and pCAL12, respectively. *E. coli* S17-1 λ*pir* was transformed with the resulting plasmids and subsequently used for conjugation. Single homologous recombination events were selected for by growth on Kan and Cm plates. To select for strains that had lost the integrated plasmid, leaving the Kan^r sequence in place of the target gene, we used sucrose selection. For sucrose selection, overnight cultures of bacteria were grown in LB broth without antibiotics, diluted, spread onto sucrose plates (5% sucrose, 8 g/liter nutrient broth, 15 g/liter agar), and then incubated for 16 h at 30°C. Sucrose-sensitive and Kan^s Cm^s strains in which the *napA* or *narZ* gene had been replaced with the Kan^r cassette were termed CAL42 and CAL34, respectively. To generate nonpolar mutants, *E. coli* S17-1 λ*pir* was transformed with either pCAL9 or pCAL10 and conjugated with CAL42 and CAL34, respectively. Sucrose selection was performed as described above, and Kan^s Cm^s strains in which the *napA* or *narZ* gene had been deleted were named CAL46 and CAL40, respectively. Nonpolar mutations were confirmed by PCR. The Δ*napA* and Δ*narZ* mutations were transiently marked with Cm^r by reintroducing pCAL9 or pCAL10 into the chromosome of CAL46 and CAL40 to create CAL117 and CAL45, respectively.

To construct the *narG* mutant CAL27, an approximately 500-bp region within the *narG* sequence was PCR amplified and digested with the restriction enzymes XbaI and SphI. The digested fragment was subsequently cloned into pGP704 and propagated in *E. coli* S17-1 λ*pir*. The resulting plasmid, pCAL5, was introduced into the IR715 chromosome by conjugation, selecting for single homologous recombination events by plating on plates containing Carb. Mutations were confirmed via PCR.

To generate a nonpolar deletion in *spiB*, *E. coli* S17-1 λ*pir* was transformed with pSPN56 and conjugated with SPN450. Integration of pSPN56 into SPN450 was selected for by plating on LB containing Cm and Nal. Sucrose selection was used to select for the loss of pSPN56. Colonies were screened for sensitivity to Cm and Kan, and a colony exhibiting both phenotypes was confirmed by PCR to contain an unmarked Δ*spiB* locus, yielding SPN456. To enable transduction of the unmarked *spiB* deletion, pSPN56 was integrated into SPN456 by conjugation as described above, resulting in a merodiploid Δ*spiB* state flanking the integrated plasmid, a state that was maintained by selection for Cm^r. A transconjugant exhibiting Cm^r and loss of the PCR product from unmarked Δ*spiB* amplification was termed SPN458 (Δ*spiB*::pSPN56).

To construct the *sopE* mutant SW976, DNA regions upstream and downstream of *sopE* were PCR amplified and digested with XbaI. The two flanking regions were ligated, PCR amplified, and cloned into pRDH10 using BamHI restriction enzyme sites to create pSW245. To create

pSW246, a Kan^r cassette was cloned into the XbaI site between the two *sopE* flanking regions in pSW245. These plasmids were conjugated from *E. coli* S17-1 λ*pir* into *S.* Typhimurium. Plasmid integration into the chromosome was verified by PCR. The *sopE* gene in SL1344 was deleted by introducing pSW246 into SL1344(pSW172) by conjugation, selecting for exconjugants on LB plates containing Carb and Kan. To ensure stable replication of the temperature-sensitive plasmid pSW172, conjugation experiments involving SL1344(pSW172) were performed at 30°C. pSW172 was subsequently cured by growth at 37°C. A Kan^r Cm^s Carb^s strain indicated that *sopE* had been replaced with Kan^r and was termed SW975.

To create a nonpolar deletion of *sopE*, pSW245 was integrated into the chromosome of SW975 by conjugation, selecting for concomitant Kan^r and Cm^r. Sucrose selection was then used to obtain a Kan^s Cm^s strain named SW976. The Δ*sopE* deletion was marked with Cm^r by conjugating SW976 with *E. coli* S17-1 λ*pir* containing pSW245. The Cm^r strain was termed CAL74.

The *narG*::pCAL5, Δ*narZ*::pCAL10, and Δ*napA*::pCAL9 mutations were transduced from CAL27, CAL45, andCAL117, respectively, into IR715. pCAL10 and pCAL9 were removed via sucrose selection, and the resulting strain was designated CAL50. The Δ*invA*::Tet^r and Δ*spiB*::pSPN56 mutations were transduced from SW562 and SPN458, respectively, into CAL50, pSPN56 was removed via sucrose selection, and the resulting strain was designated CAL87. The SopEΦ prophage from AJB719 was transduced into IR715 and CAL50 to yield strains CAL99 and CAL98, respectively. CAL63 was created by transducing the *phoN*::Kan^r mutation into SL1344. The *narG*, *napA*, and *narZ* mutations from CAL27, CAL45, and CAL117 were transduced into SL1344 and CAL63, and plasmids pCAL10 and pCAL9 were removed via sucrose selection to yield either mutants defective for a single nitrate reductase (designated CAL65, CAL51, and CAL67, respectively) or nitrate reductase-deficient mutants (CAL59 and CAL64). The *invA*::Tet^r and *spiB*::pSPN56 mutations were transduced from SW562 and SPN458 into strains CAL63 and CAL64, pSPN56 was removed via sucrose selection, and the resulting strains were designated CAL86 and CAL85, respectively. Additionally, the *sopE*::pSW245 mutation was transduced from CAL74 into strains CAL63, CAL64, CAL98, and CAL99 and the integrated plasmid pSW245 was removed via sucrose selection to create strains CAL88, CAL89, CAL102, and CAL103, respectively. The *ttrA*::pSW171 mutation was transduced from SW661 into CAL63 to yield CAL66.

Respiratory nitrate reductase assay. Bacterial overnight cultures were diluted 1:100 in LB broth containing 40 mM $NaNO_3$ and grown statically for 3 h at 37°C. The assay was performed as described previously (38). Relative nitrate reductase activity was calculated as previously described (38).

Competitive growth assays. Competition assays were performed in mucin broth containing 0.25% type II porcine mucin (Sigma-Aldrich), 40 mM morpholinepropanesulfonic acid (MOPS) buffer, trace elements (47) and magnesium sulfate (265 mg/liter) dissolved in sterile water. Sodium tetrathionate (Sigma-Aldrich) or sodium nitrate (Sigma-Aldrich) dissolved in sterile water was added at the indicated concentrations. A 1:1 ratio of two overnight bacterial strains at a final concentration of 1×10^5 CFU was used to inoculate 14 ml of mucin medium into a 15-ml screw-top conical tube. Cultures were statically incubated at 37°C for 24 h and then placed on ice. Bacterial numbers were determined by plating serial dilutions on the appropriate antibiotics. *In vitro* competition assays were performed in triplicate with different colonies.

Mouse experiments. The Institutional Animal Care and Use Committee at the University of California, Davis, approved all animal experiments. For the mouse colitis model, either wild-type C57BL/6J or iNOS-deficient B6.129P2-Nos2^{tm1Lau}/J mice (Jackson Laboratories, Bar Harbor, ME) were given streptomycin at 20 mg/mouse in 0.1 ml sterile water intragastrically 24 h prior to inoculation with bacteria as described previously (14). In competition experiments, a 1:1 ratio of competing strains at a final concentration of 1×10^8 CFU/mouse in 0.1 ml LB broth was given intragastrically. In single infections, 1×10^8 CFU/mouse of a single strain in 0.1 ml LB broth was given intragastrically. Mice were sacrificed between 1 and 4 days after infection as indicated. Cecal tissue and cecal contents were flash frozen and stored at −80°C. Colon contents were stored in phosphate-buffered saline (PBS) on ice. CFU counts were determined by plating dilutions of the inoculum or colon content on selective medium.

In the model of extended *S.* Typhimurium infection, wild-type CBA/J mice (Jackson Laboratories) were intragastrically provided an inoculum containing a 1:1 ratio of competing strains at a final concentration of 1×10^8 CFU/mouse in 0.1 ml LB broth. Fecal pellets were collected between 1 and 28 days postinfection as indicated and stored in PBS on ice. At the end of the experiment, mice were euthanized and colon contents were removed and stored in PBS on ice. CFU counts were determined by plating dilutions of the inoculum, fecal pellets, or colon content on selective medium.

Histopathology. The distal segment of the cecum was fixed in 10% buffered formalin phosphate and stained with hematoxylin and eosin. A veterinary pathologist scored histopathological changes by blinded scoring of sections by a scheme described previously (48).

Isolation of cecal RNA and proteins. Tissue was homogenized in a Mini-Beadbeater (BioSpec Products, Bartlesville, OK), and RNA and protein were isolated by the TRI-Reagent method (Molecular Research Center, Inc.) following the manufacturer's protocol. DNA remaining in the RNA isolation portion was removed using the DNA-free kit (Applied Biosystems). RNA samples and protein extracts were stored at −80°C or −20°C, respectively.

Quantification of mRNA levels. Isolated RNA was normalized to 100 ng/μl and reverse transcribed using random hexamers and Moloney murine leukemia virus reverse transcriptase (Applied Biosystems). Quantitative real-time PCR was performed using SYBR green (Applied Biosystems) PCR mix and the appropriate primer sets (see Table S2 in the supplemental material) at a final concentration of 0.25 mM. In cases where *n*-fold changes were calculated, relative expression was compared to either mock-infected cecal tissue for murine gene expression experiments or to SopE-positive *S.* Typhimurium for bacterial gene expression analysis. In cases where absolute values were calculated, a standard curve was used. To create the standards, first we used a standard PCR to amplify the target gene fragment with the quantitative reverse transcription (qRT)-PCR primers and inserting it into pCR2.1 by using the TOPO cloning kit. The resulting plasmids were sequenced. The plasmids were quantified to create a set of standards ranging from 10^8 to 10^1 copies/μl diluted in a 0.02-mg/ml yeast RNA (Sigma) solution. Each qRT-PCR was performed in duplicate.

Analysis of cecal proteins. The concentration of mouse cecal protein was measured using a Micro BCA protein assay kit (Pierce) in accordance with the manufacturer's instructions. A 0.05-mg sample of protein was separated by SDS-PAGE and transferred to a polyvinylidene fluoride membrane (Millipore). Three percent nonfat dried milk and 0.1% Tween 20 (Bio-Rad) in a PBS solution were used as blocking agents. To detect iNOS, a 1:1,500 dilution of the primary antibody (anti-mouse; BD Transduction Laboratories) in PBS with 5% bovine serum albumin (BSA) was added to the membrane. As a loading control, α/β-tubulin was detected with a 1:5,000 dilution of the primary antibody (anti-rabbit; Cell Signaling) in PBS with 5% BSA. The horseradish peroxidase (HRP)-conjugated secondary antibody (Bio-Rad), either anti-mouse or anti-rabbit, was diluted 1:5,000 in blocking buffer and applied to the membrane. Protein bands were visualized by applying 0.5 ml HRP substrate solution and imaged with a UVP BioSpectrum Imaging System. Blot density quantification was performed with the Labworks Image Acquisition and Analysis Software (UVP version 4.6.00.0).

Statistics. The natural log of the data values was calculated before statistical analysis. We used Student's *t* test to assess significance and considered *P* values below 0.05 to be significant.

SUPPLEMENTAL MATERIAL

Supplemental material for this article may be found at http://mbio.asm.org/lookup/suppl/doi:10.1128/mBio.00143-12/-/DCSupplemental.

Figure S1, PDF file, 0.1 MB.
Figure S2, PDF file, 0.1 MB.
Table S1, PDF file, 0.1 MB.
Table S2, PDF file, 0.1 MB.

ACKNOWLEDGMENTS

We acknowledge support by Public Health Service grants AI088122 and AI096528 to A.J.B. C.A.L. was supported by Public Health Service grant AI060555.

REFERENCES

1. **Anderson ES.** 1968. Drug resistance in *Salmonella typhimurium* and its implications. Br. Med. J. **3**:333–339.
2. **Rabsch W, Tschäpe H, Bäumler AJ.** 2001. Non-typhoidal salmonellosis: emerging problems. Microbes Infect. **3**:237–247.
3. **Hardt WD, Urlaub H, Galán JE.** 1998. A substrate of the centisome 63 type III protein secretion system of *Salmonella typhimurium* is encoded by a cryptic bacteriophage. Proc. Natl. Acad. Sci. U. S. A. **95**:2574–2579.
4. **Mirold S, et al.** 1999. Isolation of a temperate bacteriophage encoding the type III effector protein SopE from an epidemic *Salmonella typhimurium* strain. Proc. Natl. Acad. Sci. U. S. A. **96**:9845–9850.
5. **Ehrbar K, Hardt WD.** 2005. Bacteriophage-encoded type III effectors in *Salmonella enterica* subspecies 1 serovar Typhimurium. Infect. Genet. Evol. **5**:1–9.
6. **Hardt WD, Chen LM, Schuebel KE, Bustelo XR, Galán JE.** 1998. *S. typhimurium* encodes an activator of Rho GTPases that induces membrane ruffling and nuclear responses in host cells. Cell **93**:815–826.
7. **Hoffmann C, et al.** 2010. In macrophages, caspase-1 activation by SopE and the type III secretion system-1 of S. typhimurium can proceed in the absence of flagellin. PLoS One **5**:e12477.
8. **Müller AJ, et al.** 2009. The *S. typhimurium* effector SopE induces caspase-1 activation in stromal cells to initiate gut inflammation. Cell Host Microbe **6**:125–136.
9. **Hapfelmeier S, et al.** 2004. Role of the salmonella pathogenicity island 1 effector proteins SipA, SopB, SopE, and SopE2 in *Salmonella enterica* subspecies 1 serovar Typhimurium colitis in streptomycin-pretreated mice. Infect. Immun. **72**:795–809.
10. **Zhang S, et al.** 2002. Phage mediated horizontal transfer of the sopE1 gene increases enteropathogenicity of *Salmonella enterica* serotype Typhimurium for calves. FEMS Microbiol. Lett. **217**:243–247.
11. **Barman M, et al.** 2008. Enteric salmonellosis disrupts the microbial ecology of the murine gastrointestinal tract. Infect. Immun. **76**:907–915.
12. **Stecher B, et al.** 2007. *Salmonella enterica* serovar Typhimurium exploits inflammation to compete with the intestinal microbiota. PLoS Biol. **5**:2177–2189.
13. **Hoiseth SK, Stocker BA.** 1981. Aromatic-dependent *Salmonella typhimurium* are non-virulent and effective as live vaccines. Nature **291**:238–239.
14. **Barthel M, et al.** 2003. Pretreatment of mice with streptomycin provides a *Salmonella enterica* serovar Typhimurium colitis model that allows analysis of both pathogen and host. Infect. Immun. **71**:2839–2858.
15. **Winter SE, et al.** 2010. Gut inflammation provides a respiratory electron acceptor for salmonella. Nature **467**:426–429.
16. **Szabó C, Ischiropoulos H, Radi R.** 2007. Peroxynitrite: biochemistry, pathophysiology and development of therapeutics. Nat. Rev. Drug Discov. **6**:662–680.
17. **Barrett EL, Riggs DL.** 1982. Evidence of a second nitrate reductase activity that is distinct from the respiratory enzyme in *Salmonella typhimurium*. J. Bacteriol. **150**:563–571.
18. **Kaprálek F.** 1972. The physiological role of tetrathionate respiration in growing citrobacter. J. Gen. Microbiol. **71**:133–139.
19. **Barrett EL, Riggs DL.** 1982. *Salmonella typhimurium* mutants defective in the formate dehydrogenase linked to nitrate reductase. J. Bacteriol. **149**:554–560.
20. **Gennis RB, Stewart V.** 1996. Respiration, p 217–261. *In* Neidhardt FC et al. (ed), *Escherichia coli* and *Salmonella*: cellular and molecular biology. ASM Press, Washington, DC.
21. **McClelland M, et al.** 2001. Complete genome sequence of *Salmonella enterica* serovar Typhimurium LT2. Nature **413**:852–856.
22. **Coburn B, Li Y, Owen D, Vallance BA, Finlay BB.** 2005. *Salmonella enterica* serovar Typhimurium pathogenicity island 2 is necessary for complete virulence in a mouse model of infectious enterocolitis. Infect. Immun. **73**:3219–3227.
23. **Tsolis RM, Adams LG, Ficht TA, Bäumler AJ.** 1999. Contribution of *Salmonella typhimurium* virulence factors to diarrheal disease in calves. Infect. Immun. **67**:4879–4885.
24. **Raffatellu M, et al.** 2009. Lipocalin-2 resistance confers an advantage to *Salmonella enterica* serotype Typhimurium for growth and survival in the inflamed intestine. Cell Host Microbe **5**:476–486.
25. **Pelludat C, Mirold S, Hardt WD.** 2003. The SopEPhi phage integrates into the *ssrA* gene of *Salmonella enterica* serovar Typhimurium A36 and is closely related to the Fels-2 prophage. J. Bacteriol. **185**:5182–5191.
26. **Wood MW, Rosqvist R, Mullan PB, Edwards MH, Galyov EE.** 1996. SopE, a secreted protein of *Salmonella dublin*, is translocated into the target eukaryotic cell via a sip-dependent mechanism and promotes bacterial entry. Mol. Microbiol. **22**:327–338.
27. **Mastroeni P, et al.** 1999. Interleukin 18 contributes to host resistance and gamma interferon production in mice infected with virulent *Salmonella typhimurium*. Infect. Immun. **67**:478–483.
28. **Koide M, Kawahara Y, Nakayama I, Tsuda T, Yokoyama M.** 1993. Cyclic AMP-elevating agents induce an inducible type of nitric oxide synthase in cultured vascular smooth muscle cells. Synergism with the induction elicited by inflammatory cytokines. J. Biol. Chem. **268**:24959–24966.
29. **Koide M, Kawahara Y, Tsuda T, Yokoyama M.** 1993. Cytokine-induced expression of an inducible type of nitric oxide synthase gene in cultured vascular smooth muscle cells. FEBS Lett. **318**:213–217.
30. **Xie QW, Whisnant R, Nathan C.** 1993. Promoter of the mouse gene encoding calcium-independent nitric oxide synthase confers inducibility by interferon gamma and bacterial lipopolysaccharide. J. Exp. Med. **177**:1779–1784.
31. **Yamada K, Otabe S, Inada C, Takane N, Nonaka K.** 1993. Nitric oxide and nitric oxide synthase mRNA induction in mouse islet cells by interferon-gamma plus tumor necrosis factor-alpha. Biochem. Biophys. Res. Commun. **197**:22–27.
32. **Chiang RC, Cavicchioli R, Gunsalus RP.** 1992. Identification and characterization of narQ, a second nitrate sensor for nitrate-dependent gene regulation in *Escherichia coli*. Mol. Microbiol. **6**:1913–1923.
33. **Darwin AJ, Li J, Stewart V.** 1996. Analysis of nitrate regulatory protein NarL-binding sites in the fdnG and narG operon control regions of *Escherichia coli* K-12. Mol. Microbiol. **20**:621–632.
34. **Goh EB, et al.** 2005. Hierarchical control of anaerobic gene expression in *Escherichia coli* K-12: the nitrate-responsive NarX-NarL regulatory system represses synthesis of the fumarate-responsive DcuS-DcuR regulatory system. J. Bacteriol. **187**:4890–4899.
35. **Li J, Kustu S, Stewart V.** 1994. *In vitro* interaction of nitrate-responsive regulatory protein NarL with DNA target sequences in the fdnG, narG, narK and frdA operon control regions of *Escherichia coli* K-12. J. Mol. Biol. **241**:150–165.
36. **Stewart V.** 1982. Requirement of Fnr and NarL functions for nitrate reductase expression in *Escherichia coli* K-12. J. Bacteriol. **151**:1320–1325.
37. **Stewart V, Berg BL.** 1988. Influence of *nar* (nitrate reductase) genes on nitrate inhibition of formate-hydrogen lyase and fumarate reductase gene expression in *Escherichia coli* K-12. J. Bacteriol. **170**:4437–4444.
38. **Stewart V, Parales J, Jr..** 1988. Identification and expression of genes *narL* and *narX* of the *nar* (nitrate reductase) locus in *Escherichia coli* K-12. J. Bacteriol. **170**:1589–1597.
39. **Thauer RK, Jungermann K, Decker K.** 1977. Energy conservation in chemotrophic anaerobic bacteria. Bacteriol. Rev. **41**:100–180.
40. **Winter SE, Keestra AM, Tsolis RM, Bäumler AJ.** 2010. The blessings and curses of intestinal inflammation. Cell Host Microbe **8**:36–43.
41. **Muller L.** 1923. Un nouveau milieu d'enrichissement pour la recherche du Bacille Typhique et Paratyphique. C. R. Seances Soc. Biol. Fil. **89**:434–437.
42. **Weingarten RA, Grimes JL, Olson JW.** 2008. Role of *Campylobacter jejuni* respiratory oxidases and reductases in host colonization. Appl. Environ. Microbiol. **74**:1367–1375.
43. **Clark VL, Campbell LA, Palermo DA, Evans TM, Klimpel KW.** 1987. Induction and repression of outer membrane proteins by anaerobic growth of *Neisseria gonorrhoeae*. Infect. Immun. **55**:1359–1364.
44. **Palmer KL, Brown SA, Whiteley M.** 2007. Membrane-bound nitrate reductase is required for anaerobic growth in cystic fibrosis sputum. J. Bacteriol. **189**:4449–4455.
45. **Weber I, Fritz C, Ruttkowski S, Kreft A, Bange FC.** 2000. Anaerobic

nitrate reductase (narGHJI) activity of *Mycobacterium bovis* BCG *in vitro* and its contribution to virulence in immunodeficient mice. Mol. Microbiol. **35**:1017–1025.
46. **Vogel HJ, Bonner DM.** 1956. Acetylornithinase of *Escherichia coli*: partial purification and some properties. J. Biol. Chem. **218**:97–106.
47. **Price-Carter M, Tingey J, Bobik TA, Roth JR.** 2001. The alternative electron acceptor tetrathionate supports B12-dependent anaerobic growth of *Salmonella enterica* serovar Typhimurium on ethanolamine or 1,2-propanediol. J. Bacteriol. **183**:2463–2475.
48. **Thiennimitr P, et al.** 2011. Intestinal inflammation allows salmonella to use ethanolamine to compete with the microbiota. Proc. Natl. Acad. Sci. U. S. A. **108**:17480–17485.